Inorganic Chemistry

Article

pubs.acs.org/IC

Unusual Conformation of a Dinuclear Paddle Wheel Copper(II) Complex. Synthesis, Structural Characterization and EPR Studies

Verónica Paredes-García,*[,†,‡] Ricardo C. Santana,*[,§] Rosa Madrid,[‡] Andrés Vega,[†,‡] Evgenia Spodine,[∥,‡] and Diego Venegas-Yazigi[⊥,‡]

[†] Departamento de Ciencias Químicas, Universidad Andres Bello, Santiago, Chile

[‡]CEDENNA, Santiago, Chile

[§]Instituto de Física, Universidade Federal de Goiás, Goiânia, 74001-970, Brazil

[∥]Facultad de Ciencias Químicas y Farmacéuticas, Universidad de Chile, Santiago, Chile

[⊥]Facultad de Química y Biología, Universidad de Santiago de Chile (USACH), Santiago, Chile

Supporting Information

ABSTRACT: An unusual and unique conformation of a paddle wheel type binuclear copper(II) complex containing acetate and acetamido ligands, $\{Cu_2(\mu_2\text{-}O_2CCH_3)_4\}(OCNH_2CH_3)$ (**1**), was obtained by solvothermal synthesis. The structural characterization of this compound shows that the apical (acetamido) ligands are disposed at a 62° dihedral angle, generating a special conformation as a consequence of the synthetic method used. This conformation has not been reported in other paddle wheel copper(II) tetraacetate compounds. Electron paramagnetic resonance (EPR) spectra of powder samples of (**1**) were obtained at 9.5 and 33.8 GHz, while single crystal spectra were obtained at 33.8 GHz with a $\boldsymbol{B}_0$ applied in three orthogonal planes. The fit of the single crystal experimental data allowed gave $g_{\|} = 2.345 \pm 0.003$, and $g_{\perp} = 2.057 \pm 0.005$. The angular variation of the EPR line allows evaluation of the fine structure of (**1**), giving $D = -0.337 \pm 0.002$ cm^{-1} and $E = -0.005 \pm 0.001$ cm^{-1}. The line width angular dependence, used together with the Anderson model and Kubo−Tomita theory, permitted the interdimer interaction to be evaluated as $|J'| = (0.051 \pm 0.002)$ cm^{-1}. Using the powder spectral temperature dependence it was possible to evaluate the intradinuclear exchange coupling constan J_0 as -101 ± 2 cm^{-1}, which is considerably lower than that reported for other analogous copper(II) tetraacetate paddle wheel compounds (Cu^{II}−PW), showing the remarkable effect of the conformation of the terminal ligands on the magnetic interaction.

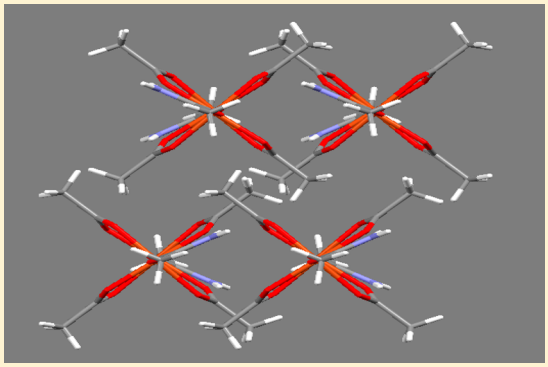

INTRODUCTION

In the past decades, thermal reactions in organic solvents (solvothermal syntheses) have been considered a good synthetic route to obtain new coordination compounds exhibiting intriguing structural diversity and properties. This synthetic technique can be carried out under relatively mild conditions at 120−200 °C, and with pressure generated exclusively by the organic medium. Although, the in situ metal/ligand reaction allows the synthesis of new products which are inaccessible or not easily obtainable by direct preparation from the ligands via conventional methods, many other new coordination compounds have been prepared taking advantage of the reactions that some of the starting materials can undergo under solvothermal conditions.[1,2] Such reactions may be, for example, the hydrolysis of carboxylate esters, organic nitriles, and amides to the corresponding carboxylates as well as decarboxylation of carboxylates among others.[3]

On the other hand, using different synthetic strategies it is also possible to obtain new and stable coordination compounds based on binuclear paddle-wheel (PW) compounds,[4,5] which have been of great interest in studying the metal−metal bond.[6] The best known PW systems contain carboxylate groups combined with other ligands coordinated to metal ions to give dimers of the type $[M(RCOO)_2L_2]_2$.[7] The interest of the PW motif is that both structural and functional changes can be achieved simply by varying the metal cores, the bridging moieties, or the ligands (L).[8] This functional versatility of the dinuclear PW motifs makes them particularly attractive for the design and synthesis of many crystalline materials ranging from zero-dimensional (0D) species to three-dimensional (3D) coordination polymers with interesting properties in areas such as magnetism,[9] catalysis,[10] and gas storage.[11]

From the magnetic point of view, since Bleaney−Bowers,[12] Guha[13] and Doedens[14] reported the magnetic characterization of copper acetates, dinuclear compounds with polyatomic bridging ligands have been studied uninterruptedly. Electron Paramagnetic Resonance (EPR) spectroscopy has also been

Received: December 18, 2012
Published: July 24, 2013

   dx.doi.org/10.1021/ic3027804 | Inorg. Chem. 2013, 52, 8369−8377

used as a powerful technique to investigate binuclear units,[15−19] because it allows the magnitude of small exchange interactions (J') between neighboring binuclear units, and the isotropic exchange coupling (J_0) between two unpaired spins within the binuclear unit, to be selectively measured even at high temperatures or weak magnetic fields. Furthermore, single crystal EPR characterization of binuclear copper(II) systems is also interesting because it is possible to observe and characterize the abrupt transition from a phase where the spectra are clearly resolved and dominated by the anisotropic spin−spin interactions to a phase where this interaction is collapsed. In this work we present the structural and single crystal electron paramagnetic resonance characterization of a Cu^{II}−PW compound of the type $\{Cu_2(\mu_2\text{-}O_2CCH_3)_4\}(OCNH_2CH_3)_2$, which exhibits an unusual conformation of the axial ligands. This Cu^{II}−PW compound was obtained by solvothermal synthesis and contains important hydrogen bonds, both intra- and intermolecular, which give it special structural features. To the best of our knowledge the synthesis and structural characteristics of this dinuclear copper(II) complex have not been previously reported.

EXPERIMENTAL DETAILS

Synthesis and Crystallization of $\{Cu_2(\mu_2\text{-}O_2CCH_3)_4\}(OCNH_2CH_3)_2$ (1). All reagents and solvents were of p.a. quality, and used without any previous purification process. Compound **1** was obtained by the solvothermal method from L-phenylalanine and $Cu(NO_3)_2{\cdot}4H_2O$ which were used in a 2:3 molar ratio, in a mixture of $CH_3CN/CH_3CH_2OH/H_2O$ (3:5:7) as solvent. All components were placed in a 23 mL Teflon-lined stainless steel autoclave vessel, and the reaction mixture was heated at 130 °C for 24 h under self-generated pressure. After slow cooling (0.05 °C/min) to room temperature, the reaction mixture was left approximately for one month at room temperature, depositing greenish blue rhombohedral single crystals of $\{Cu_2(\mu_2\text{-}O_2CCH_3)_4\}(OCNH_2CH_3)_2$. X-ray diffraction quality crystals (Supporting Information, Figure 1S) were directly separated from the bulk material. This reaction was performed many times, and the same crystalline product was always obtained. Yield 78%. Anal. Calcd. for $C_{12}H_2N_2O_{10}Cu_2$: C: 29.94; H: 4,57; N: 5,82. Found: C: 29.91; H: 4.39; N: 5.93%.

Single-Crystal X-ray Diffraction. The crystal structure of **1** was determined at 150 K by X-ray diffraction measurements on a prismatic 0.54 × 0.28 × 0.14 mm^3 single crystal. Data collection was run on a SMART CCD diffractometer, using ω-scans. Data reduction was done with SAINT,[20] while the structure solution by direct methods; completion and refinement was conducted with SHELXL.[21] Multiscan absorption corrections were applied using SADABS.[22] The hydrogen atom positions were calculated after each cycle of refinement with SHELXL, using a riding model for each structure, with a C−H distance of 0.98 Å and N−H distance of 0.88 Å. $U_{iso}(H)$ values were set equal to 1.2 U_{eq} of the parent carbon atom (1.9 U_{eq} for methyl). Additional data collection and refinement details are given in Table 1.

EPR Spectra. EPR spectra of finely powdered samples of **1** were collected at temperatures between 4 and 300 K with an ELEXSYS E-580 spectrometer working at ∼9.47 GHz (X-band), while EPR experiments at the Q-band (∼33.8 GHz) were performed with a Bruker ESP-300E spectrometer at room temperature, using powder and single crystal samples. EPR spectra of a single crystal sample were obtained with the applied magnetic field oriented in all three orthogonal planes, using intervals of 5° and covering a range of 180°. In the zone of the ac^* and bc^* planes, close to the magic angles, the interval used was 0.5°. The magnetic field at the position of the sample was calibrated using 2,2-diphenyl-1-picrylhydrazyl (dpph, g = 2.0036) as the field marker. The positions of the axes in the crystalline planes were determined within 1° from the symmetry properties of the crystal axes. The positions of the a, b, and c^* axes in the ac^* and bc^* planes were accurately determined considering the $C2/c$ symmetry of the spectra around the b-axis. The positions of the c^* and a axes in the ac^* plane were determined by comparison with results in the other planes. The EasySpin package,[23] which works under the Matlab platform,[24] was used for spectral simulations.

Table 1. Crystal Data and Structure Refinement Details for $\{Cu_2(\mu\text{-}O_2CCH_3)_4\}(OCNH_2CH_3)_2$ (1)

FW/uma	481.42
crystal system	monoclinic
space group	$C2/c$
a/Å	15.466(2)
b/Å	9.667(1)
c/Å	14.675(2)
β/deg	119.874(2)
V/Å^3	1902.5(4)
Z (Z')	4(4)
δ/g cm^{-3}	1.681
μ/mm^{-1}	2.29
F(000)	984.0
θ range	2.6 to 25.0
hkl range	h: −18 →18
	k: −11→11
	l: −17→17
N_{tot}, N_{uniq}	5677, 1676
(R_{int}), N_{obs}	(0.071), 1578
refinement parameters	121
GOF	1.15
R1, wR2 (obs)	3.92,11.52
R1, wR2 (all)	4.06,11.58
max. and min $\Delta\rho$	1.22 and −0.62

RESULTS AND DISCUSSION

Synthesis. Compound $\{Cu_2(\mu_2\text{-}O_2CCH_3)_4\}(OCNH_2CH_3)_2$, which contains acetate and acetamide as ligands, was obtaining from L-phenylalanine and $Cu(NO_3)_2{\cdot}4H_2O$. No source of acetate or acetamide was used in the solvothermal synthesis. Therefore, the presence of these ligands in the reported product should be explained by the decomposition of some initial component. Similar evidence of this decomposition was given in previous work, where compounds $Na_3[Mn_3(HCOO)_9]$[25] and *cis*-$[Ni(\mu\text{-ox})(H_2O)_2]_\infty$[26] were obtained under similar experimental conditions and with similar starting materials. In these previous papers, although no source of formate or oxalate was used, these anions appear in the final reported compounds. In both cases, the use of the amino acid during the synthesis is crucial, as no $Na_3[Mn_3(HCOO)_9]$ or *cis*-$[Ni(\mu\text{-ox})(H_2O)_2]_\infty$ were obtained without its use. The same is true for compound $\{Cu_2(\mu_2\text{-}O_2CCH_3)_4\}(OCNH_2CH_3)_2$: if L-phenylalanine was not used as a starting reagent, no crystalline product was obtained. Furthermore, using similar experimental conditions but with acetamide as reagent, $\{Cu_2(\mu_2\text{-}O_2CCH_3)_4\}(OCNH_2CH_3)_2$ is not obtained.

The evidence obtained for the previously reported compounds $Na_3[Mn_3(HCOO)_9]$ and *cis*-$[Ni(\mu\text{-ox})(H_2O)_2]_\infty$,[25,26] suggests that the presence of formate and oxalate in these complexes should be due to the decomposition of the amino acid serine. Depending on the nature of the metal ion different ligand species were obtained. However, for the compound reported in this work, the amino acid L-serine was replaced by L-phenylalanine, and the solvent DMF was replaced by a mixture of $CH_3CN/CH_3CH_2OH/H_2O$. Under these different synthetic conditions the final product also contains a

dx.doi.org/10.1021/ic3027804 | Inorg. Chem. 2013, 52, 8369−8377

ligand which was not used as an initial reagent. This fact can be explained using the mechanism reported in the literature, in which nitriles in aqueous medium can be converted, by two successive hydration reactions, to amides and then to ammonia and carboxylate (Scheme 1).[27]

Scheme 1. Hydrolysis Reactions of Nitrile Groups

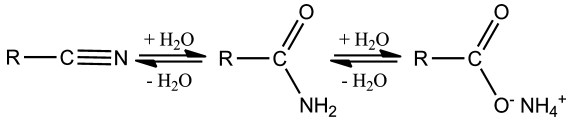

Therefore, the presence of acetate and acetamido ligands in $\{Cu_2(\mu_2\text{-}O_2CCH_3)_4\}(OCNH_2CH_3)_2$ can be attributed to the hydrolysis reaction of acetonitrile, which can be converted into the acetamido and acetate ligands. Moreover, this reported synthetic procedure can be considered as an alternative route to generate new Cu^{II}–PW compounds based on different carboxylate and amide ligands, depending of the chemical characteristic of the nitriles used as starting materials. It is important to remark, again, that the use of the amino acid is crucial, as no crystalline product is obtained in its absence. The experimental evidence allows to infer a key role for the amino acid, probably forming a "precursor complex species" which undergoes the subsequent transformations.

Structural Description. The title compound $\{Cu_2(\mu\text{-}O_2CCH_3)_4\}(OCNH_2CH_3)_2$ has the typical structure of the widely known copper carboxylates, with a central $Cu_2(\mu\text{-}O,O'\text{-}O_2CR)_4$ core. This arrangement displays each cupric center surrounded by four oxygen atoms from four different carboxylate molecules, allowing a rather short intermetallic distance, typically around 2.6 Å (2.6092(9) Å for **1**), and leaving two axial positions available for terminal ligands, as depicted in Scheme 2. These axial positions can be chemically

Scheme 2. Arrangement of $\{Cu_2(\mu\text{-}O_2CCH_3)_4\}(OCNH_2CH_3)_2$

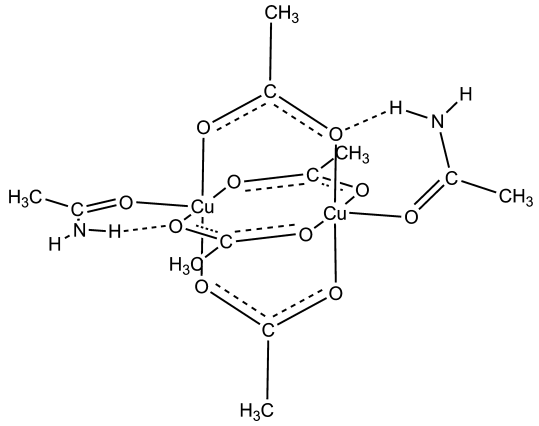

substituted, leading to an entire family of compounds of the type $\{Cu_2(\mu\text{-}O_2CCH_3)_4\}L_2$. For the case when L is a multidentate ligand, different molecular and multidimensional structures can be obtained.[28]

It is usually seen in the crystal structures of these compounds that L tends to adopt a staggered conformation between the copper oxygen bonds. That conformation is easily explained in terms of the steric interaction between both fragments in the complex. An exception occurs when L is able to form a hydrogen bond with the carboxylate oxygen atoms, leading to an eclipsed conformation.[29] The structure of $\{Cu_2(\mu\text{-}O_2CCH_3)_4\}(OCNH_2CH_3)_2$ (Scheme 2 and Figure 1) falls within this last kind of complexes.

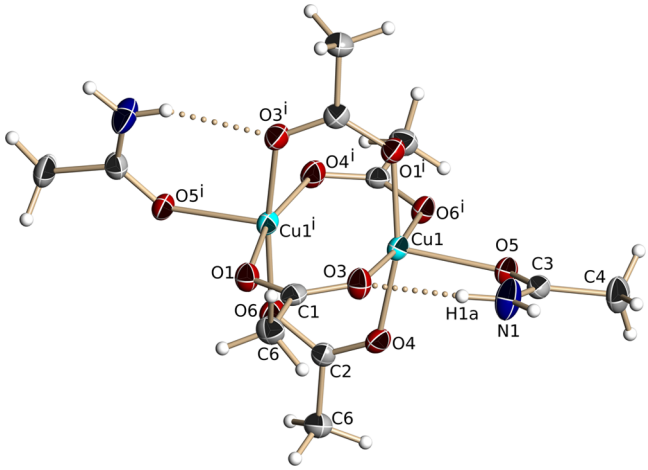

Figure 1. Molecular structure diagram for $\{Cu_2(\mu\text{-}O_2CCH_3)_4\}(OCNH_2CH_3)_2$ showing a partial numbering scheme, and intramolecular hydrogen bonds. Hydrogen atoms are drawn as spheres of arbitrary radius. Symmetry label: ^{i} $-x, y, -z + 3/2$.

An intramolecular hydrogen bond between one of the amide hydrogen atoms (H1a) and an acetate oxygen atom (O3) defines an interaction with an N···O distance equal to 2.969(5) Å (See Figure 1). This is reflected in the low value measured for the Cu1–O5–C3-N1 torsion angle, 5.8(6)° (Table 2). Contrarily to what is observed for the derivatives where L is urea or acetic acid, the planes which contain both apical molecules form a dihedral angle between the least-squares planes defined by O5, C3, C4, and N1 and $O5^{i}$, $C3^{i}$, $C4^{i}$, and $N1^{i}$ of 61.9(2)° (i: $-x, y, -z + 3/2$). The molecule has a C_2 as symmetry point group. This makes this structure a conformer of that previously reported by Trivedi et al.,[30] $\{Cu_2(\mu\text{-}O_2CCH_3)_4\}(OCNH_2CH_3)_2$, where the acetamide molecules adopt an anti conformation, defining a dihedral angle of 180° and making the molecule centrosymmetric. To the best of our knowledge no other similar situation has been previously reported for $\{Cu_2(\mu\text{-}O_2CCH_3)_4\}L_2$ complexes. The hydrogen atom not involved in the intramolecular interaction, H1b, interacts with a carboxylate oxygen atom (O6) of a neighboring molecule ($-x, y, -z + 3/2$), as shown in Figure 2, defining an intermolecular hydrogen bond with N···O equal to 3.002(5) Å (Table 3). Although both the intramolecular and the intermolecular hydrogen bonds are also present in the conformer reported by Trivedi et al.,[30] with N···O equal to 2.946(5) Å and 3.066(2) Å, respectively, the different mutual orientations of the acetamide molecules lead to very different packing patterns. Figure 2 presents the possible Cu(II)–Cu(II) superexchange paths, connecting neighboring copper ions from dinuclear units, spatially separated by 7.0448(9) Å. These paths are formed by equatorial–apical carboxylate bonds of the *syn–anti* type, $-Cu1-O5ap-C3-N1-H1B\cdots-O6^{ii}eq-Cu1^{ii}-$ (ii: $-x+1/2, y+1/2, -z+3/2$), resulting in zigzag infinite chains along the *a* axis. Considering all bonds, the total length of this path is 9.663 Å.

EPR Spectra of Powder Samples at 300 K. The powder EPR spectra of **1** recorded at 300 K for the Q- and X-bands are

dx.doi.org/10.1021/ic3027804 | Inorg. Chem. 2013, 52, 8369–8377

Table 2. Selected Bond and Interatomic Distances (Å), Bond and Torsion Angles (deg) for $\{Cu_2(\mu\text{-}O_2CCH_3)_4\}(OCNH_2CH_3)_2$[a]

O1—C1	1.262 (5)	O1—Cu1^{i}	1.985 (3)
Cu1—O3	1.960 (3)	O6—Cu1^{i}	1.963 (3)
Cu1—O6^{i}	1.963 (3)	Cu1—O1^{i}	1.985 (3)
Cu1—O4	1.988 (3)	Cu1—O5	2.134 (3)
Cu1···Cu1^{i}	2.6092(9)		
O3—Cu1—O1^{i}	89.73 (13)	O6^{i}—Cu1—O1^{i}	89.18 (12)
O3—Cu1—O4	89.58 (13)	O6^{i}—Cu1—O4	89.49 (13)
O1^{i}—Cu1—O4	165.56 (11)	O3—Cu1—O5	98.48 (12)
O6^{i}—Cu1—O5	89.52 (11)	O1i—Cu1—O5	99.96 (11)
O4—Cu1—O5	94.40 (11)		
Cu1—O5—C3—N1	5.8(6)	Cu1—O5—C3—C4	−175.5(3)

[a]Symmetry label: ^{i} $-x, y, -z + 3/2$.

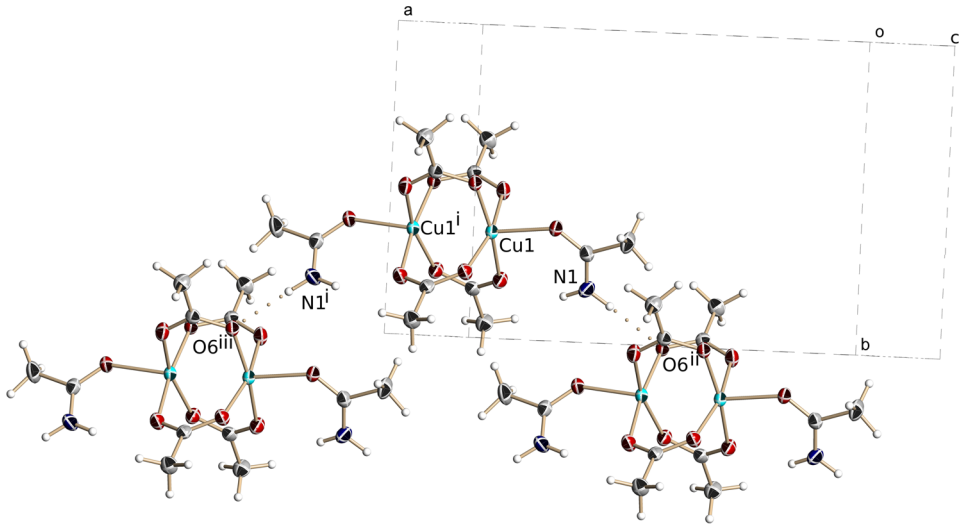

Figure 2. Packing diagram for $\{Cu_2(\mu\text{-}O_2CCH_3)_4\}(OCNH_2CH_3)_2$ showing the intermolecular hydrogen bonds. Hydrogen atoms are drawn as spheres of arbitrary radius. Symmetry labels: ^{i} $-x, y, -z + 3/2$; ^{ii} $-x + 1/2, y + 1/2, -z + 3/2$; ^{iii} $-x - 1/2, y + 1/2, -z + 3/2$.

Table 3. Hydrogen-Bond Geometry (Å, deg)[a]

D—H···*A*	—H	···*A*	*D*···*A*	*D*—H···*A*
N1—H1*a*···O3	0.88	0.17	2.969(5)	150
N1—H1B···O6^{ii}	0.88	0.14	3.002(5)	166

[a]Symmetry label: ^{ii} $x + 1/2, y + 1/2, z$.

shown in Figures 3a and 3b, respectively. The spectra are typical spectra for isolated dinuclear units with the B_{z1}, B_{x1y1}, B_{x2y2}, and B_{z2} peaks labeled according to the standard notation.[31−34] In the Q-band spectrum (Figure 3a) peak B_{z2} is superimposed on the stronger peak B_{x2y2}, and the signal at ∼519 mT corresponds to the forbidden transition $S_z = +1 \leftrightarrow -1$ ($\Delta M = \pm 2$), that in the X-band overlaps the B_{z1} transition. At low T (Figure 3b) peak B_{z1} at 22 mT should display a hyperfine structure, which is produced by the interaction of the unpaired electron with two copper nuclei within the dinuclear unit.[16,33,34] However, in the studied case these signals are not obvious because of the poor resolution of the transitions. The large B_{x2y2} signal at 472 mT (Figure 3b), is narrow and splits into two components, B_{x2} (453 mT) and B_{y2} (486 mT), when the temperature is lowered. The origin of this behavior has been attributed to the rhombic deviation of the structure from axial symmetry. Similar results were also reported by Kozlevčar et al.,[34,35] for copper dinuclear compounds. No signals of dinuclear units are observed below 25 K as a consequence of the depopulation of the $S = 1$ magnetic state in the copper dinuclear units.

The narrow peaks at 1203 mT (Q-band) and 338 mT (X-band) arise from the dpph marker. In addition, the powder spectra display, at both frequencies, intense and wide central peaks at 1102 and 317 mT (heretofore called "U" peaks) which are not expected for a dinuclear unit. Moreover, these peaks are too strong to be attributed to contamination with paramagnetic mononuclear spins, and their intensities decrease with the lowering of temperature, as is to be expected for dinuclear components. At lower temperatures ($T < 150$ K), the intensity of the U peak decreases allowing the signals designated as M to be observed in the range of 250 to 330 mT, which are attributed to mononuclear Cu^{II} ions.[36] The M signals show a characteristic powder spectrum of monomeric Cu^{II} ions, where the well resolved hyperfine lines originate by the interaction of the electron spin ($S = 1/2$) with the nuclear spin ($I = 3/2$). Furthermore, as expected for mononuclear Cu^{II} ions, the intensity increases with decreasing temperature (see Figure 3b). The fit of the experimental EPR spectra for the uncoupled dinuclear compound was done using the following spin Hamiltonian (eq 1)[37]

$$\mathcal{H}_0 = -J_0[S(S+1)/2 - 3/4] + (\mathbf{S}\cdot\boldsymbol{D}\cdot\mathbf{S} - \mathbf{s}\cdot\boldsymbol{D}\cdot\mathbf{s}) + \mu_B(\mathbf{S}\cdot\mathbf{g}_0 + \mathbf{s}\cdot\boldsymbol{G})\cdot\boldsymbol{B}_0 \quad (1)$$

dx.doi.org/10.1021/ic3027804 | Inorg. Chem. 2013, 52, 8369−8377

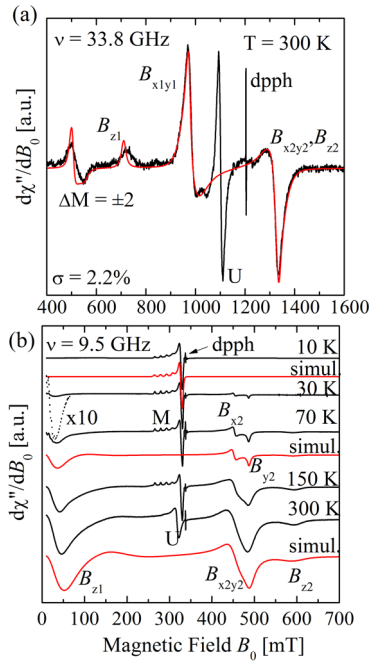

Figure 3. EPR powder spectra of (**1**) recorded at (a) Q-band at room temperature and (b) X-band at different temperatures. Black lines are experimental results, and red lines correspond to simulated spectra (10, 70, and 300 K). The rms deviations for calculated spectra in (b) are 0.5%, 1.0%, and 5.0% for 10 K, 70 K, and 300 K, respectively.

where

$$\mathbf{g}_0 = (\mathbf{g}_1 + \mathbf{g}_2)/2, \quad \mathbf{S} = \mathbf{S}_1 + \mathbf{S}_2, \quad \mathbf{D} = \mathbf{D}_{12}/2$$

$S_1 = S_2 = 1/2$ for copper(II) ions, J_0 is the isotropic Heisenberg exchange interaction, and $\boldsymbol{D}$ is the symmetric matrix considering the dipole−dipole anisotropic exchange contribution to the zero field splitting. In the case when the spin coupling between neighboring units is neglected, the following spin Hamiltonian can be used,

$$\mathcal{H}_0 = \mathbf{S}\cdot\mathbf{D}\cdot\mathbf{S} + \mu_B(\mathbf{S}\cdot\mathbf{g}_0\cdot\mathbf{B}_0) \quad (2)$$

The best fits of the powder spectra lead to values of $g_\parallel$ = 2.345 ± 0.004, $g_\perp$ = 2.057 ± 0.003 with axial and rhombic zero field splitting parameters D = (−0.334 ± 0.003) cm^{-1} and E = (0.010 ± 0.002) cm^{-1}, respectively. The sign of D could not be obtained from the EPR experiments, but was taken from the results obtained for other reported tetracarboxylate Cu^{II}−PW.[38] The simulations obtained with the values given above are shown as dashed lines in Figure 3b, and are in good agreement with the experimental spectra (except in the U or M peak field ranges, where the fit was not attempted). The obtained parameters are similar to those reported for analogous Cu^{II} dimers.[34,35] The M peaks were also fitted using the EasySpin program,[23] and the experimental data can be fitted using the spin Hamiltonian:

$$\mathcal{H}_S = \mu_B\mathbf{S}\cdot\mathbf{g}\cdot\mathbf{B}_0 + \mathbf{S}\cdot\mathbf{A}\cdot\mathbf{I} \quad (3)$$

where μ_B is the Bohr magneton, $\mathbf{S}$ = 1/2 is the effective electronic spin operator, $\boldsymbol{g}$ is the crystal g-matrix, considering that the principal directions of the g-matrix and those of the angular variation of the line width are the same, $\boldsymbol{A}$ is the hyperfine coupling, and $\boldsymbol{I}$ = 3/2 is the nuclear spin operator for Cu^{II}. The principal components of the g- and A-matrices, obtained from the fittings of the powder spectra at 10 K, are $g_\parallel$ = 2.369 ± 0.002, $g_\perp$ = 2.073 ± 0.001, $A_\parallel$ = (154 ± 2) × 10^{-4} cm^{-1}, $A_\perp \approx 0$ cm^{-1}, and the calculated spectra are in good agreement with the experimental spectra.

From the temperature variation experiments we calculated a normalized intensity ratio $R(T)$ between the integrated area of the signal B_{z1} and that of the signal corresponding to the dpph marker, as a function of T, and the result is displayed as $T \times R(T)$ vs T in Figure 4. Following the procedure described by

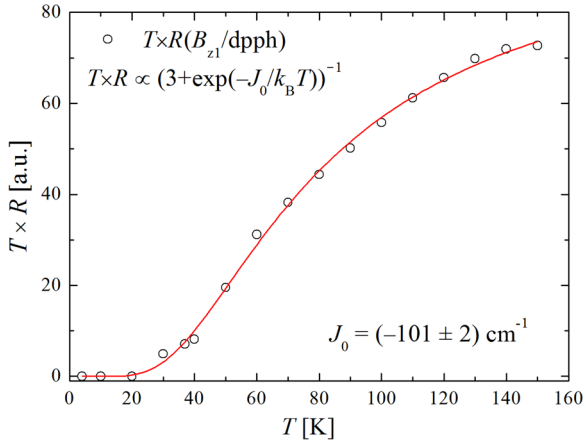

Figure 4. Temperature variation of the ratio (R) between the integrated areas of the spectra at the X-band of the dinuclear peak B_{z1} and the dpph marker multiplied by T. The solid line is the best fit to the data, using the Bleaney−Bowers equation, as explained in the text.

Napolitano et al.,[19] it was possible to calculate the exchange parameter J_0, using the Bleaney−Bowers equation, which considered the exchange coupling between Cu^{II} ions with spins $\mathbf{S}_1$ and $\mathbf{S}_2$ defined as $\mathcal{H}_{ex} = -J_0\,\boldsymbol{S}_1\cdot\boldsymbol{S}_2$,[12,15,19,39]

$$T \times R(T) = \frac{1}{3 + \exp(-J_0/k_BT)} \quad (4)$$

where k_B is the Boltzmann constant and T is the temperature. A least-squares fit of the experimental data using eq 4, gives J_0 = −101 ± 2 cm^{-1}, with statistical coefficient r = 0.9984.

The powder EPR results are typical of isolated dinuclear species, in which a classical triplet state of Cu^{II} can be observed. Compound **1** is also characterized by a large tetragonal zero-field parameter, and by presenting a well resolved Cu^{II} monomer signal at T < 150 K. The intradinuclear exchange coupling J_0 of −101 ± 2 cm^{-1} can be compared with the values found for other reported dinuclear compounds, which are given in Table 4.[17,19−40] The obtained J_0 value for (**1**) is significantly lower compared with the reported intradinuclear exchange values for Cu^{II}−PW with different −O−C−O− bridges (Table 4, compounds (6)−(12)).[42−47] The antiferromagnetic exchange coupling observed for (**1**) is also greater than the value measured for dinuclear compounds with two carboxylate groups (Table 4, compounds (2)−(5)),[19,40,41] corroborating that decreasing antiferromagnetic interactions can be related to the decrease of the number of the carboxylates bridging copper ions.[48] The Cu−O−C−O−Cu bridge (φ_{bend}), the oxygen ligand at the axial positions, the dihedral angle between Cu−O−O−Cu and the carbonyl moiety, are parameters which can contribute to a decrease of the exchange parameter because of the poor overlap of the Cu $d_{x^2-y^2}$ orbital with the $2p_x$ carboxylate oxygen orbital.[10g]

dx.doi.org/10.1021/ic3027804 | Inorg. Chem. 2013, 52, 8369−8377

Table 4. Magnetic Parameters for 1 and for Other Dinuclear Cu^{II} Compounds[a]

compound	Cu···Cu (Å)	g_{iso}[b]	$\|D\|$ (cm^{-1})	J_0 (cm^{-1})	J' (cm^{-1})	ref.
1	2.609(2)	2.153(3)	0.333(3)	−101(2)	0.051(2)	t.w.
$Cu_2[TzTs]_4$ (**2**)	2.786(2)	2.112(2)	0.198(3)	−113(1)	0.060(15)	19
$Cu_2ac_2phen_2$ (**3**)	3.063(3)	2.136(5)	0.128(3)	−74(3)	0.04(1)	39, 40
$Cu(Sal{\cdot}N{\cdot}p\text{-}tol)C_2H_5CO_2$ (**4**)	3.122(1)	2.14		−50.5		41
$Cu_2fo_2phen_2$ (**5**)	3.103(2)	2.18	0.156(2)	−62.5		40
$Cu_2(dpda)(dpdo)$ (**6**)	2.7797(4)	2.13(0)		−120.2439(7)		42
$[Cu_2(Indo)_4(DMF)_2]$ (**7**)	2.630(1)	2.16	0.341(1)	−152.5(1)		43
$[Cu_2(flu)_4(dmf)_2]$ (**8**)	2.619	2.17	0.334(1)	−294(5)	0.005	44
$Cu_2(GAA)_4(NO_3)_2$ (**9**)	2.65		0.3(0.01)	−134.5(2)		7k
$[Cu(2\text{-butenoate})_2]_n$ (**10**)	2.5765(8)	2.217(5)	0.329(3)	−330.6(1)		45
$Cu(C_{10}H_6O_6)(H_2O)$ $1.66H_2O$ (**11**)	2.6212(3)	2 0.16 (0.01)	0.337 (0.001)	−167(4)		46
$Cu_2(CH_3COO)_4(H_2O)_2$ (**12**)	2.09			−296		17, 47

[a] $Cu_2[TzTs]_4$ = [*N*-thiazol-2-yltoluenesulfonamidatecopper(II)]; $Cu_2ac_2phen_2$ = $[(CH_3COO)(1,10\text{-phenanthroline})(H_2O)]_2{\cdot}(NO_3)_2{\cdot}4H_2O$; $Cu_2(Sal\text{-}N\text{-}p\text{-}tol)C_2H_5CO_2$ = di-μ-propionato-*O*,*O*′-bis[*N*-*p*-tolylsalicylideaminatocopper(II)]; $Cu_2fo_2phen_2$ = $[Cu(HCOO)(1,10\text{-phenanthroline})(H_2O)]_2(NO_3)_2{\cdot}4H_2O$; $Cu_2(dpda)(dpdo)$ = $[Cu_2(2,2'\text{-biphenyldicarboxylate})_2(H_2O)_2(4,4'\text{-dipyridine-}N,N'\text{-dioxide})0.5]_n$; $[Cu_2(Indo)4(DMF)_2]$ = Bis(*N*,*N*′-dimethylformamide)tetrakis-μ-(*O*,*O*′-indo)dicopper-(II)1.6-*N*,*N*′-Dimethylformamide; $[Cu_2(flu)4(dmf)_2]$ = tetrakis(μ_2-*N*-3-trifluoromethyl phenylanthranilato-*O*,*O*′)-bis(dimethylformamide)-di-copper(II);$Cu_2(GAA)_4(NO_3)_2$ = tetrakis(l-guanidinoacetic acid) bis[(nitrato) copper-(II);$[Cu(2\text{-butenoate})_2]_n$; $Cu(C_{10}H_6O_6)(H_2O)$ $1.66H_2O$ = (1,3,5-benzenetricarboxylate) (H_2O); $Cu_2(CH_3COO)_4(H_2O)_2$. [b] $g_{iso} = (g_{\|} + 2g_{\perp})/3$.

Single Crystal EPR Spectra. Spectra of single crystals of **1**, measured at room temperature with the Q-band in the *bc** plane, and for selected angles (near the magic angle at 57° with the *c** axis), are displayed in Figure 5. Similar spectra are obtained for the *ac** plane. Depending on the magnetic field orientation the spectra show one or two peaks which correspond to the allowed $S_z = 0 \leftrightarrow \pm 1$ transitions. The sharpness and sudden collapse of the resonances observed in the single crystal EPR spectra arise from the anisotropic spin−spin coupling between the neighboring dinuclear units, which can also be interpreted as a dimensional quantum phase transition between a 0-dimensional binuclear unit and a 1D spin chain.[39] A third resonance line at ≈524 mT ($g \approx 4.6$), was observed for most angles, and should correspond to the *forbidden* transition $S_z = \pm 1 \leftrightarrow \mp 1$,[49] but is outside of the field of these figures. In the *ab* plane, the two resonances corresponding to the allowed transitions do not change with the angle. In all planes and for any orientation of the magnetic field, no hyperfine splitting is resolved. The B_0 positions and Γ widths were obtained fitting the line derivative shapes of the experimental spectra with one or two Lorentzian functions. Figure 6 shows the fitting results for B_0, which correspond to typical coupled copper(II) centers with spin $S = 1$, displaying a dipolar type angular variation described by $f(\theta) \approx 1/2\ (3\cos^2\theta - 1)$, where $\theta = 0$ corresponds to the axial direction of the dinuclear units.[39] It is possible to observe that when B_0 is parallel to the *c** axis in the *ac** and *bc** planes the maximum splitting occurs between the allowed transitions. The angular variation of the positions was obtained from eq 2, as results of the fit of the experimental data and based on the procedure described by Napolitano et al.[19] and Calvo et al.[39] The best fit was obtained with the following parameters $g_{\|} = 2.345 \pm 0.003$, $g_{\perp} = 2.057 \pm 0.005$, $D = -0.337 \pm 0.002$ cm^{-1}, and $E = -0.005 \pm 0.001$ cm^{-1} (Figure 6). In the fit the angular regions near the *magic angles* (where the fine structure peaks are collapsed) were not considered, and a good agreement factor between theoretical and experimental data was obtained ($\sigma = 2.5$). As

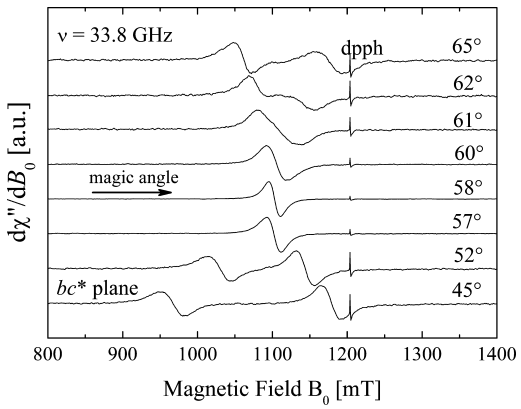

Figure 5. Selected EPR spectra of compound **1** measured in the *bc** plane, showing the collapse of the lines at the magic angle at room temperature.

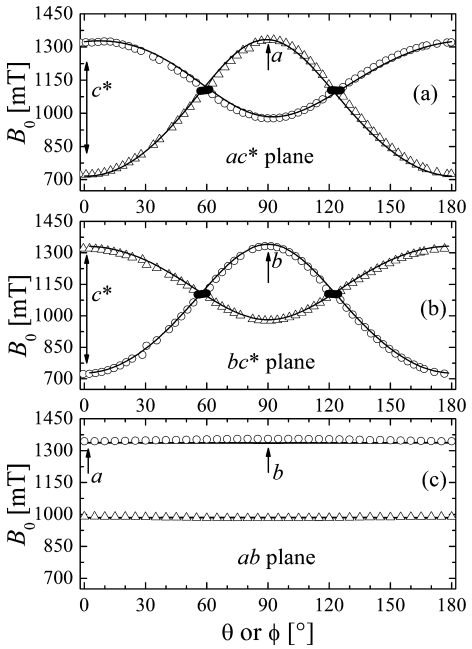

Figure 6. Angular dependence of the allowed $S_z = 0 \leftrightarrow \pm 1$ transitions observed with B_0 in the (a) *ac**, (b) *bc**, and (c) *ab* planes. Symbols and the solid lines are experimental and fitting data, respectively.

dx.doi.org/10.1021/ic3027804 | *Inorg. Chem.* 2013, 52, 8369−8377

expected, the additional U-peak which appears in the powder spectra is not reproduced in the calculated data.

The peak-to-peak widths of the $S_z = 0 \leftrightarrow \pm 1$ transitions observed in the *bc** plane are displayed in Supporting Information, Figure 2S. The plots show a significant narrowing in the regions where the lines collapse (magic angles). The angular variation widths obtained in the *ac** plane are similar to those obtained in the *cb** plane. Since the widths obtained in the *ab* plane do not give any relevant information, these are not presented here. A very interesting experimental fact was obtained from the collapse region (black symbols in Supporting Information, Figure 2S). A significantly lesser narrowing is observed for (**1**) as compared to the results obtained by single crystal EPR experiments for other recently reported dinuclear compounds (see refs 19 and 42). From the collapsed resonance width (Γ_{obs}) as a function of the magnetic field orientation (see Supporting Information, Figure 3S) it was possible to evaluate the exchange coupling between neighboring binuclear units from the equation

$$\Gamma_{obs} = \frac{g\mu_B(\Delta B_0^{calc})^2}{\hbar\omega_{ex}} + \Gamma_0 \qquad (5)$$

based on the Anderson and Weiss theory,[50,51] giving a mean value of $\hbar\omega_{ex} = (0.088 \pm 0.004)$ cm^{-1}. ΔB_0^{calc} in eq 5 is the splitting of the collapsing resonances calculated in the absence of exchange interactions which can be extracted from the solid lines plotted in Figure 6. Γ_0 is a residual contribution to the line width arising from other broadening sources, considered here as a constant. This approach has been successfully used to study the collapse of EPR signals arising from mononuclear and dinuclear units.[19,37,52]

The plot of the ratio *R*, between the experimental and calculated splittings of the fine structure ($R = \Delta B_0^{exp}/\Delta B_0^{calc}$) as a function of the inverse of the calculated splitting is shown in Figure 7. When $(\Delta B_0^{calc})^{-1}$ is large, close to the magic angles, the signals are collapsed and $R = 0$. Far from the magic angles, $(\Delta B_0^{calc})^{-1}$ is small and $R \approx \pm 1$. The collapse is abrupt and occurs when $g\mu_B[\Delta B_0^{calc}]_{collapse} = \hbar\omega_{ex}$, a condition which allows the exchange frequency ω_{ex} to be obtained. From the fit of the experimental data using eq 6, it is possible to calculate the average value of $\hbar\omega_{ex(collapse)} = (0.056 \pm 0.002)$ cm^{-1}.

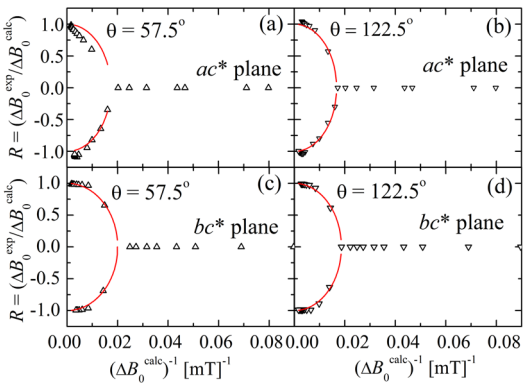

Figure 7. Plot of the *R* ($R = \Delta B_0^{exp}/\Delta B_0^{calc}$) ratio as a function of $(\Delta B_0^{calc})^{-1}$, where the ΔB_0^{exp} and ΔB_0^{calc} are the observed and calculated splittings of the fine structure peaks calculated in the neighborhood of the magic angles in the *ac** and *bc** planes. The symbols and solid lines correspond to the experimental results and the fitting values, respectively.

$$R = \frac{\Delta B_0^{calc}}{\Delta B_0^{calc}} = \pm\sqrt{1 - \left(\frac{\hbar\omega_{ex}}{g\mu_B\Delta B_0^{calc}}\right)^2} \qquad (6)$$

From the two methods described above, an average of the values of the exchange frequencies is $\hbar\omega_{ex} = (0.072 \pm 0.003)$ cm^{-1}. Napolitano et al.[19] and Passeggi et al.[53] have pointed that when $\hbar\omega_{ex}$ is obtained at room temperature, where $k_BT \gg J_0$, the relationship $2|J'|^2 \approx \hbar^2\omega_{ex}^2$ can be used to obtain $|J'|$, the value being 0.051 ± 0.002 cm^{-1} between neighboring dinuclear units for the studied system. The internuclear coupling was calculated from the single crystal EPR experiments, based on the general theories of magnetic resonance, and Anderson's and Kubo's models for exchange narrowing.[50,51,54]

The internuclear coupling $|J'| = (0.051 \pm 0.002)$ cm^{-1} evaluated here is supported by the type of chemical paths between the dinuclear units, with five diamagnetic atoms (9.663 Å) and one O···H−N hydrogen bond (see the crystallographic section). Our result is of the same order of magnitude, within experimental error, as that found for the dinuclear compound $Cu_2[TzTs]_4$,[19] where the path contains the same number of diamagnetic atoms and a weak hydrogen bond, and those reported for $Cu_2ac_2phen_2$,[40] and $[Cu_2(flu)_4(dmf)_2]$.[44] The sign of J' cannot be obtained from the EPR results.

The principal values of the *g*-tensor, where the $g_{\parallel} > g_{\perp}$ pattern indicates a $d_{x^2-y^2}$ ground state orbital, and the values of the axial, $D = -0.337 \pm 0.002$ cm^{-1}, and rhombic, $E = 0.005 \pm 0.001$ cm^{-1}, zero-field splitting parameters of the $S = 1$ triplet state were evaluated. The *D*-term arises from intradinuclear dipole−dipole and anisotropic exchange ($D = D_{dip} + D_{exch}$). The dipole−dipole contribution to the zero-field splitting is related to the Cu···Cu distance, and can be estimated by the relationship: $D_{dip} = -0.65/R^3\{(g_{\parallel})^2 + 0.5(g_{\perp})^2\}$,[48] where *R* is the Cu···Cu separation (2.609 Å in the studied system), resulting in $D_{dip} = -0.279$ cm^{-1}, and $D_{exch} = -0.054$ cm^{-1}. These results compare well with those found for dinuclear copper(II) complexes with carboxylate bridges and axial symmetry reported in the literature for other dinuclear compounds.[43,45,55−57] An inspection of Table 4 reveals that for compounds with double carboxylate bridges[19,40,41] the *D* parameter is significantly lower than that obtained for tetracarboxylate compounds.

Finally, with respect to the U peak that was observed in the powder spectra of (**1**), the origin of this peak was attributed to the collapse of the fine structure around the magic angles, because of the interactions between the binuclear units and the simultaneous narrowing of the collapsed line in the single crystal spectra.[39,45] Supporting Information, Figure 4S displays the powder spectra and the observed angular variation of the positions of the resonances taken at the same frequencies and *T*, corroborating the above hypothesis.

CONCLUSIONS

Through the solvothermal conditions, and in the presence of an amino acid as precursor, it was possible to obtain an unexpected and unusual conformation of the Cu^{II}−PW dinuclear compound based on acetate and acetamido ligands, $\{Cu_2(\mu_2\text{-}O_2CCH_3)_4\}(OCNH_2CH_3)$. This special conformation is not a random product, because it was obtained as the major crystalline product from different batches. Furthermore, to the best of our knowledge this conformation has not been previously reported for Cu^{II}−PW binuclear compounds.

dx.doi.org/10.1021/ic3027804 | Inorg. Chem. 2013, 52, 8369−8377

$\{Cu_2(\mu_2\text{-}O_2CCH_3)_4\}(OCNH_2CH_3)$ was structurally and magnetically characterized using EPR spectroscopy. Through the powder and single crystal EPR measurements it was possible to evaluate the magnetic exchange couplings and the fine structure parameters. The intradinuclear exchange coupling of -101 cm^{-1} is smaller than that observed in other Cu^{II}−PW binuclear units, probably because of the poor overlap of the Cu $d_{x^2-y^2}$ orbital with the $2p_x$ carboxylate oxygen orbitals. Thus not only the nature of the ligands (L) but also the molecular conformation are important factors that determine the J value. The interdinuclear coupling ($|J'| = (0.051 \pm 0.002)$ cm^{-1}) between the dinuclear units is consistent with the number of diamagnetic atoms and hydrogen bonds participating in the chemical paths bridging the dinuclear units. The very small value obtained for the interdinuclear interaction shows clearly how powerful the EPR technique can be for the characterization of extremely small J values contributing, for example, to an understanding of the most efficient pathways for these small magnetic interactions in biological systems.

■ ASSOCIATED CONTENT

Supporting Information

Crystallographic data in CIF format. Further details are given in Figures 1S−4S. This material is available free of charge via the Internet at http://pubs.acs.org.

■ AUTHOR INFORMATION

Corresponding Author

*E-mail: vparedes@unab.cl (V.P.G.), santana@if.ufg.br (R.C.S.). Phone: +56-2-2770-3434 (V.P.G.), +55-62-3521-1014 (R.C.S.).

Notes

The authors declare no competing financial interest.

■ ACKNOWLEDGMENTS

The authors acknowledge financial support from FONDECYT 1090477 and Proyecto Basal CEDENNA, Financiamiento Basal FB0807 in Chile, and from the Conselho Nacional de Desenvolvimento Científico e Tecnológico (CNPq) in Brazil (Project 471146/2010-2). Thanks are given to the Consejo Superior de Investigaciones Científicas (CSIC) of Spain for the award of a license for the use of the Cambridge Crystallographic Data Base (CSD). The authors are grateful to O. R. Nascimento (IFSC-USP) for allowing us to perform EPR measurements in the range 4−150 K.

■ REFERENCES

(1) (a) Fang, S,-M.; Chen, M.; Yang, X.-G.; Hu, J.-Y.; Liu, Ch.-S. *Inorg. Chem. Commun.* **2012**, *22*, 101. (b) Coskun, A.; Hmadeh, M.; Barin, G.; Gándara, F.; Li, Q.; Choi, E.; Strutt, N. L.; Cordes, D. B.; Slawin, A. M. Z.; Stoddart, J. F.; Sauvage, J.-P.; Yaghi, O. M. *Angew. Chem., Int. Ed.* **2012**, *51*, 2204. (c) He, Y.; Zhang, Z.; Xiang, S.; Wu, H.; Fronczek, F. R.; Zhou, W.; Krishna, R.; O'Keeffe, M.; Chen, B.-L. *Chem.—Eur. J.* **2012**, *18*, 1901. (d) Wang, G.-H.; Lei, Y.-Q.; Wang, N.; He, R.-L.; Jia, H.-Q.; Hu, N.-H.; Xu, J.-W. *Cryst. Growth Des.* **2010**, *10*, 534.

(2) (a) Chen, X.-M.; Tong, M.-L. *Acc. Chem. Res.* **2007**, *40*, 162. (b) Zhang, X.-M. *Coord. Chem. Rev.* **2005**, *249*, 1201. (c) Duriska, M. B.; Batten, S. R.; Price, D. J. *Aus. J. Chem.* **2006**, *59*, 26. (d) Du, M.; Zhao, X.-J.; Batten, S. R.; Ribas, J. *Cryst. Growth. Des.* **2005**, *5*, 901. (e) Matsuda, R.; Kitaura, R.; Kitigawa, S.; Kubota, Y.; Kobayashi, T. C.; Horike, S.; Takata, M. *J. Am. Chem. Soc.* **2004**, *126*, 14063. (f) Bu, X.-H.; Tong, M.-L.; Chang, H.-C.; Kitigawa, S.; Batten, S. R. *Angew. Chem., Int. Ed.* **2003**, *43*, 192. (g) Cordes, D. B.; Sharma, C. V. K.; Rogers, R. *Cryst. Growth Des.* **2007**, *7*, 1943.

(3) (a) Li, G.-B.; Liu, J.-M.; Yu, Z.-Q.; Wang, W.; Su, C.-Y. *Inorg. Chem.* **2009**, *48*, 8659. (b) Wang, W.-J.; Xu, L.; Gao, G.-G.; Liu, X. Z. *Inorg. Chem. Commun.* **2011**, *14*, 594. (c) Kanoo, P.; Haldar, R.; Cyriac, S. T.; Maji, T. K. *Chem. Commun.* **2011**, *47*, 11038. (d) Feller, R. K.; Forster, P. M.; Wudl, F.; Cheetham, A. K. *Inorg. Chem.* **2007**, *46*, 8717. (e) Lü, J.; Han, L.-W.; Lin, J.-X.; Cao, R. *Cryst. Growth Des.* **2011**, *11*, 2035. (f) Zheng, Y.-Z.; Tong, M.-L.; Chen, X.-M. *J. Mol. Struct.* **2006**, *796*, 9. (g) Nadeem, M. A.; Bhadbhade, M.; Bircher, R.; Stride, J. A. *Cryst. Growth Des.* **2010**, *10*, 4060. (h) Li, Y.; Xu, G.; Zou, W.-Q.; Wang, M.-S.; Zheng, F.-K.; Wu, M.-F.; Zeng, H.-Y.; Guo, G.-C.; Huang, J.-S. *Inorg. Chem.* **2008**, *47*, 7945. (i) Qiu, Y.-C.; Li, Y.-H.; Peng, G.; Cai, J.-B.; Jin, L.-M.; Ma, L.; Deng, H.; Zeller, M.; Batten, S. R. *Cryst. Growth Des.* **2010**, *10*, 1332. (j) Cheng, L.; Zhang, W.-X.; Ye, B.-H.; Lin, J.-B.; Chen, X.-M. *Inorg. Chem.* **2007**, *46*, 1135. (k) Li, C.-P.; Zhao, X.-H.; Chen, X.-D.; Yu, Q.; Du, M. *Cryst. Growth Des.* **2010**, *10*, 5034. (l) Hix, G. B.; Kariuki, B. M.; Kitchin, S.; Tremayne, M. *Inorg. Chem.* **2001**, *40*, 1477. (m) Tong, M.-L.; Li, L.-J.; Mochizuki, K.; Chang, H.-C.; Chen, X.-M.; Li, Y.; Kitagawa, S. *Chem. Commun.* **2003**, 428.

(4) (a) Marques, L. F.; Marinho, M. V.; Correa, C. C.; Speziali, N. L.; Diniz, R.; Machado, F. C. *Inorg. Chim. Acta* **2011**, *368*, 242. (b) Xu, W.; Zheng, Y.-Q. *J. Chem. Crystallogr.* **2012**, *42*, 313. (c) Song, Y. J.; Kwak, H.; Lee, Y. M.; Kim, S. H.; Lee, S. H.; Park, B. K.; Jun, J. Y.; Yu, S. M.; Kim, C.; Kim, S.-J.; Kim, Y. *Polyhedron* **2009**, *28*, 1241. (d) Aakeröy, C. B.; Scott, B. M. T.; Smith, M. M.; Urbina, J. F.; Desper, J. *Inorg. Chem.* **2009**, *48*, 4052. (e) Lu, J. Y. *Coord. Chem. Rev.* **2003**, *246*, 327.

(5) (a) Guo, X. G.; Yang, W. B.; Wu, X. Y.; Zhang, K.; Lin, L.; Yu, R. M.; Lu, C. Z. *CrystEngComm* **2013**, *15*, 3654. (b) Aakeröy, C. B.; Schultheiss, N.; Desper, J. *Dalton. Trans.* **2006**, 1627. (c) Su, S. Q.; Wang, S.; Song, X. Z.; Song, S. Y.; Qin, C.; Zhu, M.; Hao, Z. M.; Zhao, S. N.; Zhang, H. J. *Dalton Trans.* **2012**, *41*, 4772. (d) Park, I.-H.; Lee, S. S.; Vittal, J. J. *Chem.—Eur. J.* **2013**, *19*, 2695.

(6) Cotton, F. A., Murillo, C. A., Walton, R. A., Eds.; *Multiple Bonds between Metal Atoms*, 3rd ed.; Springer: New York, 2005.

(7) (a) MacGillivray, L. In *Metal-Organic Frameworks: Design and Application*; John Wiley and Sons: New York, 2010. (b) Meek, S. T.; Greathouse, J. A.; Allendorf, M. D. *Adv. Mater.* **2011**, *23*, 249. (c) Köberl, M.; Cokoja, M.; Hermann, W. A.; Kühn, F. E. *Dalton Trans.* **2011**, *40*, 6834. (d) Carné, A.; Carbonell, C.; Imaz, I.; Maspoch, D. *Chem. Soc. Rev.* **2011**, *40*, 291. (e) Mas-Ballesté, R.; Gómez-Herrero, J.; Zamora, F. *Chem. Soc. Rev.* **2010**, *39*, 4220. (f) Givaja, G.; Amo-Ochoa, P.; Gómez-García, C. J.; Zamora, F. *Chem. Soc. Rev.* **2012**, *41*, 115. (g) Pérez-Yáñez, S.; Beobide, G.; Castillo, O.; Cepeda, J.; Luque, A.; Román, P. *Cryst. Growth Des.* **2012**, *12*, 3324. (h) Pasynskii, A. A.; Shapovalov, S. S.; Gordienko, A. V.; Razuvaev, D. I.; Skabitsky, I. V.; Aleksandrov, G. G.; Dobrohotova, Z. W.; Bogomyakov, A. S. *Inorg. Chim. Acta* **2012**, *384*, 18. (i) Amirjalayer, S.; Tafipolsky, M.; Schmid, R. J. *Phys. Chem. C* **2011**, *115*, 15133. (j) He, R.; Song, H. H.; Wu, L. L.; Wei, Z.; Wang, T. *Chin. J. Chem.* **2011**, *28*, 898. (k) Miranda, J. L.; Felcman, J.; Herbst, M. H.; Vugman, N. V. *Inorg. Chem. Commun.* **2008**, *11*, 655.

(8) (a) Leong, W. L.; Vittal, J. J. *Chem. Rev.* **2011**, *111*, 688. (b) Vagin, S. I.; Ott, A. K.; Rieger, B. *Chem. Ing. Tech.* **2007**, *79*, 767. (c) Chen, B.; Xiang, S.; Quian, G. *Acc. Chem. Res.* **2010**, *43*, 1115. (d) Zhao, D.; Timmons, D. J.; Yuan, D.; Zhou, H. C. *Acc. Chem. Res.* **2011**, *44*, 123.

(9) (a) Li, H. J.; Yao, H. C.; Zhang, E. P.; Jia, Y. Y.; Hou, H. W.; Fan, Y. T. *Dalton Trans.* **2011**, *40*, 9388. (b) Manna, P.; Tripuramallu, B. K.; Das, S. K. *Cryst. Growth Des.* **2012**, *12*, 4607. (c) Chang, X. H.; Ma, L. F.; Hui, G.; Wang, L. Y. *Cryst. Growth Des.* **2012**, *12*, 3638. (d) Wang, X. Z.; Zhu, D. R.; Xu, Y.; Yang, J.; Shen, X.; Zhou, J.; Fei, N.; Ke, X. K.; Peng, L. M. *Cryst. Growth Des.* **2010**, *10*, 887. (e) Sen, R.; Hazra, D. K.; Koner, S.; Helliwell, M.; Mukherjee, M.; Bhattacharjee, A. *Polyhedron* **2010**, *29* (17), 3183. (f) Bernini, M. C.; Platero-Prats, A. E.; Snejko, N.; Gutierrez-Puebla, E.; Labrador, A.;

Saez-Puche, R.; de Paz, J. R.; Monge, M. A. *CrystEngComm* **2012**, *14*, 5493.
(10) (a) Shi, D.; Ren, Y.; Jiang, H.; Cai, B.; Lu, J. *Inorg. Chem.* **2012**, *51*, 6498. (b) Wang, F.; Kang, Y. *Inorg. Chem. Commun.* **2012**, *20*, 266. (c) Kanoo, P.; Gurunatha, K. L.; Maji, T. K. J. *Mater. Chem.* **2010**, *20*, 1322. (d) Agterberg, F. P. W.; Kluit, H. A. J. P.; Driessen, W. L.; Reedijk, J.; Oevering, H.; Buijs, W.; Veldman, N.; Lakin, M. T.; Spek, A. L. *Inorg. Chim. Acta* **1998**, *267*, 183. (e) Matsunaga, S.; Hasada, K.-I.; Sugiura, K.; Kitamura, N.; Kudo, Y.; Endo, N.; Mori, W. *Bull. Chem. Soc. Jpn.* **2012**, *85*, 433438. (f) Sarma, D.; Ramanujachary, K. V.; Stock, N.; Natarajan, S. *Cryst. Growth Des.* **2011**, *11*, 1357. (g) Agterberg, F. P. W.; Kluit, H. A. J. P.; Driessen, W. L.; Oevering, H.; Buijs, W.; Lakin, M. T.; Spek, A. L.; Reedijk, J. *Inorg. Chem.* **1997**, *36*, 4321.
(11) (a) Ling, Y.; Yang, F. L.; Deng, M. L.; Chen, Z. X.; Liu, X. F.; Weng, L. H.; Zhou, Y. M. *Dalton Trans.* **2012**, *41*, 4007. (b) Dey, R.; Haldar, R.; Maji, T. K.; Ghoshal, D. *Cryst. Growth Des.* **2011**, *11*, 3905. (c) Tan, K.; Nijem, N.; Canepa, P.; Gong, Q.; Li, J.; Thonhauser, T.; Chabal, Y. J. *Chem. Mater.* **2012**, *24*, 3153. (d) Gomez, D. A.; Combariza, A. F.; Sastre, G. *Phys. Chem. Chem. Phys.* **2012**, *14*, 2508. (e) Murray, L. J.; Dinca, M.; Yano, J.; Chavan, S.; Bordiga, S.; Brown, C. M.; Long, J. R. *J. Am. Chem. Soc.* **2010**, *132*, 7856.
(12) Bleaney, B.; Bowers, K. D. *Proc. Roy. Soc. (London)* **1952**, *214*, 451.
(13) Guha, B. C. *Proc. Roy. Soc. A (London)* **1951**, *206*, 353.
(14) Doedens, R. J. *Prog. Inorg. Chem.* **1976**, *21*, 209.
(15) Bencini, A.; Gatteschi, D. *Electron Paramagnetic Resonance of Exchange Coupled Systems*; Springer-Verlag: Berlin, Germany, 1990.
(16) Pilbrow, J. R. *Transition Ion Electron Paramagnetic Resonance*; Clarendon Press: Oxford, U.K., 1990.
(17) Kahn, O. *Molecular Magnetism*; VCH: New York, 1993.
(18) Calvo, R. *Appl. Magn. Reson.* **2007**, *31*, 271.
(19) Napolitano, L. M. B.; Nascimento, O. R.; Cabaleiro, S.; Castro, J.; Calvo, R. *Phys. Rev. B* **2008**, *77*, 214423.
(20) *SAINT-NT*; Bruker AXS Inc.: Madison, WI, 1999.
(21) Sheldrick, G. M. *SHELXL-97, Program for Crystal Structure Refinement*; University of Göttingen: Göttingen, Germany, 1997.
(22) *SMART-NT and SADABS*; Bruker AXS Inc.: Madison, WI, 2001.
(23) Stoll, S.; Schweiger, A. *J. Magn. Reson.* **2006**, *178*, 42.
(24) *MatLab*; The MathWorks, Inc.: Natick, MA, 2002.
(25) Paredes-Garcia, V.; Vega, A.; Novak, M. A.; Vaz, M. G. F.; Souza, D. A.; Spodine, E. *Inorg. Chem.* **2009**, *48*, 4737.
(26) Paredes-Garcia, V.; Rojas, I.; Venegas-Yazigi, D.; Spodine, E.; Resende, J. A. L. C.; Vaz, M. G. F.; Novak, M. A. *Polyhedron* **2011**, *30*, 3171.
(27) (a) Izzo, B.; Klein, M. *Ind. Eng. Chem. Res.* **1999**, *38*, 1183. (b) Krümer, A.; Mittelstädt, S.; Vogel, H. *Chem. Eng. Technol.* **1998**, *21*, 494. (c) Duan, P.-G.; Li, S.; Wang, Z. Z.; Dai, L. Y. *Chem. Eng. Res. Des.* **2010**, *88*, 1067.
(28) (a) Zhu, L.-N.; Gao, S.; Huo, L.-H.; Xuebao, W. H. *Chin. J. Inorg. Chem.* **2008**, *24*, 670. (b) Liu, Y.; Yan, P.-F.; Yu, Y.-H.; Hou, G.-F.; Gao, J.-S.; Lu, J. Y. *Cryst. Growth Des.* **2010**, *10*, 1559. (c) Wang, X.-L.; Chen, B.-K.; Lin, H.-Y.; Hu, H.-L.; Li, J. *Transition Met. Chem.* **2009**, *34*, 307. (d) Olguin, J.; Castillo, A.; Gomez-Vidales, V.; Hernandez-Ortega, S.; Toscano, R. A.; Munoz, E.; Castillo, I. *Supramol. Chem.* **2009**, *21*, 502. (e) Li, X.-Y.; Liu, L.-Q.; Ma, M.-L.; Zhao, X.-L.; Wen, K. *Dalton Trans.* **2010**, *39*, 8646. (f) Ryan, P. E.; Lescop, C.; Laliberte, D.; Hamilton, T.; Maris, T.; Wuest, J. D. *Inorg. Chem.* **2009**, *48*, 2793. (g) Shahid, M.; Mazhar, M.; O'Brien, P.; Afzaal, M.; Raftery, J. *Acta Crystallogr., Sect. E: Struct.Rep. Online* **2009**, *65*, m163. (h) Barquin, M.; Garmendia, M. J. G.; Larrinaga, L.; Pinilla, E.; Seco, J. M.; Torres, M. R. *J. Coord. Chem.* **2010**, *63*, 1652. (i) Hu, H.-L.; Suen, M.-C.; Yeh, C.-W.; Chen, J.-D. *Polyhedron* **2005**, *24*, 1497. (j) Boonmak, J.; Youngme, S.; Chaichit, N.; van Albada, G. A.; Reedijk, J. *Cryst. .Growth Des.* **2009**, *9*, 3318. (k) Fischer, N. V.; Alam, M. S.; Jumh, I.; Stocker, M.; Fritsch, N.; Dremov, V.; Heinemann, F. W.; Burzlaff, N.; Muller, P. *Chem.—Eur. J.* **2011**, *17*, 9293.
(29) (a) Rao, M.; Sathyanarayana, D. N.; Manohar, H. *J. Chem. Soc., Dalton Trans.* **1983**, 2167. Uekusa, H.; Ohba, S.; Saito, Y.; Kato, M.; Tokii, T.; Muto, Y. *Acta Crystallogr., Sect. C: Cryst. Struct. Commun.* **1989**, *45*, 377. Vives, G.; Mason, S. A.; Prince, P. D.; Junk, P. C.; Steed, J. W. *Cryst. Growth Des.* **2003**, *3*, 699.
(30) Trivedi, M.; Nagarajan, R.; Kumar, A.; Molloy, K.; Kociok-Köhn, G.; Sudlow, A. L. *Inorg. Chem. Commun.* **2011**, *14*, 920.
(31) Atherton, N. M. *Principles of Electron Spin Resonance*; Ellis Horwood; PTR Prentice Hall: New York, 1993.
(32) Weil, J. A. Bolton, J. R. *Electron Paramagnetic Resonance: Elementary Theory and Practical Applications*; Wiley-Interscience: New York, 2007.
(33) Wasserman, E.; Snyder, L. C.; Yager, W. A. *J. Chem. Phys.* **1964**, *41*, 1763.
(34) Kozlevčar, B.; Šegedin, P. *Croat. Chem. Acta* **2008**, *81*, 369.
(35) Kozlevčar, B.; Leban, I.; Petrič, M.; Petriček, S.; Roubeau, O.; Reedijk, J.; Šegedin, P. *Inorg. Chim. Acta* **2004**, *357*, 4220.
(36) Smith, T. D.; Pilbrow, J. R. *Coord. Chem. Rev.* **1974**, *13*, 173.
(37) Weil, J. A. *EPR Newslett.* **2007**, *17*, 1.
(38) Ozarowski, A. *Inorg. Chem.* **2008**, *47*, 9760.
(39) Calvo, R.; Abud, J.; Sartoris, R. P.; Santana, R. C. *Phys. Rev. B* **2011**, *84*, 104433.
(40) Tokii, T.; Watanabe, N.; Nakashima, M.; Muto, Y.; Morooka, M.; Ohba, S.; Saito, I. *Bull. Chem. Soc. Jpn.* **1990**, *63*, 364.
(41) Tokii, T.; Emori, S.; Muto, Y. *Bull. Chem. Soc. Jpn.* **1974**, *47*, 2887.
(42) Yin, P.-X.; Zhang, J.; Li, Z.-J.; Cheng, J.-K.; Qin, Y.-Y.; Zhang, L.; Yao, Y.-G. *Inorg. Chim. Acta* **2007**, *360*, 3525.
(43) Weder, J. E.; Hambley, T. W.; Kennedy, B. J.; Lay, P. A.; MacLachlan, D.; Bramley, R.; Delfs, C. D.; Murray, K. S.; Moubaraki, B.; Warwick, B.; Biffin, J. R.; Regtopm, H. L. *Inorg. Chem.* **1999**, *38*, 1736.
(44) Nascimento, O. R.; Napolitano, L. M. B.; Torre, M. H.; Peña, O.; Calvo, R. *J. Braz. Chem. Soc.* **2011**, *22*, 669.
(45) Perec, M.; Baggio, R.; Sartoris, R. P.; Santana, R. C.; Peña, O.; Calvo, R. *Inorg. Chem.* **2010**, *49*, 695.
(46) El Mkami, H.; Mohideen, M. I. H.; Pal, C.; McKinlay, A.; Scheimann, O.; Morris, R. E. *Chem. Phys. Lett.* **2012**, *544*, 17.
(47) Martin, R. L. In *New Pathways in Inorganic Chemistry*; Ebsworth, E. A. V., Maddock, A., Sharpe, A., Eds.; Cambridge University Press: Cambridge, U.K., 1968.
(48) Rodríguez-Fortea, A.; Alemanym, P.; Alvarez, S.; Ruíz, E. *Chem.—Eur. J.* **2001**, *7*, 627.
(49) Sebastian, S. E.; Harrison, N.; Batista, C. D.; Balicas, L.; Jaime, M.; Sharma, P. A.; Kawashima, N.; Fisher, I. R. *Nature* **2006**, *441*, 617.
(50) Anderson, P. W.; Weiss, P. R. *Rev. Mod. Phys.* **1953**, *25*, 269.
(51) Anderson, P. W. *J. Phys. Soc. Jpn.* **1954**, *9*, 316−339.
(52) (a) Martino, D. M.; Passeggi, M. C. G.; Calvo, R. *Phys. Rev. B* **1995**, *52*, 9466. (b) Martino, D. M.; Passeggi, M. C. G.; Calvo, R.; Nascimento, O. R. *Phys. B* **1996**, *225*, 63.
(53) Passeggi, M. C. G.; Calvo, R. *J. Magn. Reson. Ser. A* **1995**, *114*, 1.
(54) (a) Kubo, R.; Tomita, K. *J. Phys. Soc. Jpn.* **1954**, *9*, 888. (b) Kubo, R. In *Stochastic Processes in Chemical Physics, Advances in Chemical Physics*; Schuler, K. E., Ed.; Wiley: New York, 1969; Vol. *XV*, p 101. (c) Kubo, R.; Toda, M.; Hashitsume, N. *Statistical Physics II. Nonequilibrium Statistical Mechanics*; Springer: Berlin, Germany, 1978.
(55) Chasteen, N. D. *Inorg. Chem.* **1971**, *10*, 2339.
(56) Schlam, R. F.; Perec, M.; Calvo, R.; Lezama, L.; Insausti, M.; Rojo, T.; Foxman, B. M. *Inorg. Chim. Acta* **2000**, *310*, 81.
(57) Boonmak, J.; Youngme, S.; Chaichit, N.; van Albada, G. A.; Reedijk, J. *Cryst. Growth Des.* **1999**, *38*, 1736.